JPET Fast Forward. Published on November 15, 2005 as DOI: 10.1124/jpet.105.094599

JPET #94599

Title Page

Modulation of Expression of Rat Mitochondrial 2-Oxoglutarate Carrier in NRK-52E Cells Alters Mitochondrial Transport and Accumulation of Glutathione and Susceptibility to Chemically Induced Apoptosis

Feng Xu, David A. Putt, Larry H. Matherly, and Lawrence H. Lash

Department of Pharmacology (F.X, D.A.P., L.H.M. L.H.L.) and

Experimental and Clinical Therapeutics Program,

Barbara Ann Karmanos Cancer Institute (L.H.M.)

Wayne State University School of Medicine

Detroit, Michigan 48201

Running Title Page

Running Title:

Modulation of Renal Mitochondrial GSH Transport

Author to Whom Correspondence Should be Addressed:

Lawrence H. Lash, Ph.D.

Department of Pharmacology

Wayne State University School of Medicine

540 East Canfield Avenue

Detroit, MI 48201

Phone: (313)-577-0475; FAX: (313)-577-6739; E-mail: l.h.lash@wayne.edu

Manuscript Information:

Text Pages = 35

Number of Tables = 2

Number of Figures = 9

Number of References = 41

Number of Words in Abstract = 241

Number of Words in Introduction = 675

Number of Words in Discussion = 1538

Abbreviations: rDIC, rat dicarboxylate carrier; DCVC, *S*-(1,2-dichlorovinyl)-L-cysteine; FACS, flow activated cell sorting; wild-type NRK-52E cells, NRK-52E-WT; rOGC, rat 2-oxoglutarate carrier; rOGC-C221,224S; rOGC containing C-to-S mutations at positions 221 and 224; PBS, phosphate-buffered saline; PhSucc, phenylsuccinate; tBH, *tert*-butyl hydroperoxide; TMD, transmembrane domain.

Recommended Section Assignment: Toxicology

Abstract

We previously showed that two anion carriers of the mitochondrial inner membrane, the dicarboxylate carrier (DIC; *Slc25a10*) and oxoglutarate carrier (OGC; *Slc25a11*), transport glutathione (GSH) from cytoplasm into mitochondrial matrix. In the previous study, NRK-52E cells, derived from normal rat kidney proximal tubules, were transfected with the wild-type cDNA for the DIC expressed in rat kidney; DIC transfectants exhibited increased mitochondrial uptake and accumulation of GSH and were markedly protected from chemically induced apoptosis. In the present study, cDNAs for both wild-type (WT) and a double-cysteine mutant of rat OGC (rOGC and rOGC-C221,224S, respectively) were expressed in *E. coli*, purified, and reconstituted into proteoliposomes to assess their function. While both WT rOGC and rOGC-C221,224S exhibited transport properties for GSH and 2-oxoglutarate that were similar to those found in mitochondria of rat kidney proximal tubules, rates of transport and mitochondrial accumulation of substrates were reduced by > 75% in rOGC-C221,224S as compared to the WT carrier. NRK-52E cells were stably transfected with the cDNA for WT-rOGC and exhibited 10- to 20-fold higher GSH transport activity than non-transfected cells and were markedly protected from apoptosis induced by *tert*-butyl hydroperoxide (tBH) or *S*-(1,2-dichlorovinyl)-L-cysteine (DCVC). In contrast, cells stably transfected with the cDNA for rOGC-C221,224S were not protected from tBH- or DCVC-induced apoptosis. These results provide further evidence that genetic manipulation of mitochondrial GSH transporter expression alters mitochondrial and cellular GSH status, resulting in markedly altered susceptibility to chemically induced apoptosis.

Introduction

The mitochondrial pool of GSH in cells such as hepatocytes and renal proximal tubular cells is critical for regulation of thiol and redox status, cellular energetics, and as part of the process involved in induction of apoptosis (Beatrice et al., 1984; Kroemer et al., 1998; Lê-Quôc and Lê-Quôc, 1985; Reed, 1990; Yagi and Hatefi, 1984). Although free GSH is present at similar millimolar concentrations in both the mitochondrial matrix and cytoplasm, the mitochondrial GSH pool is not passively regulated. Because there is little if any *de novo* synthesis of GSH within the mitochondria (Griffith and Meister, 1985; Lash et al., 1998), the mitochondrial GSH pool must be derived from transport of GSH from the cytoplasm across the mitochondrial inner membrane (Smith et al., 1996).

Initial investigations of mitochondrial GSH transport in liver or kidney focused on the relationship between transport activity and energetics (Griffith and Meister, 1985; Martensson and Meister, 1989; Schnellmann, 1991). Our first approach towards understanding mitochondrial GSH transport began with the realization that GSH is an anion and, hence, may be a substrate for one or more of the various anion carriers of the mitochondrial inner membrane (McKernan et al., 1991). Several of the anion carriers share a common 30 kDa molecular weight subunit and are believed to belong to a carrier "superfamily" (Palmieri et al., 1996). Substrates for these various carriers include inorganic phosphate, citric acid cycle metabolites, and glycolytic intermediates such as lactate and pyruvate. We demonstrated an important role for two of the carriers from rat kidney mitochondria, the dicarboxylate carrier (DIC; *Slc25a10*) and oxoglutarate carrier (OGC; *Slc25a11*), in GSH transport by assessments of substrate specificities, patterns of inhibition, and energetics in suspensions of isolated mitochondria from rat renal cortical homogenates, isolated rat proximal tubular cells, and partially purified and reconstituted carrier proteins from rabbit kidney mitochondria (Chen and Lash, 1998; Chen et al., 2000; Lash et al., 1998; McKernan et al., 1991).

Both the DIC and OGC proteins have been purified to homogeneity and reconstituted into proteoliposomes (Bisaccia et al., 1985, 1988; Kaplan and Pedersen, 1985; Lançar-Benba et

al., 1994). Two difficulties with studying the purified DIC protein from mammalian tissues relate to its low abundance in the inner mitochondrial membrane and its instability in its purified form, due to autoxidation and inactivation (Bisaccia et al., 1988; Kaplan and Pedersen, 1985). To circumvent this limitation, the cDNA for the DIC from Norway rat was isolated using related expressed sequence tags (ESTs) homologous to genes in *Caenorhabditis elegans* and yeast (Kakhniashvili et al., 1997). The rat DIC was then expressed in *E. coli* and functionally reconstituted into proteoliposomes (Fiermonte et al., 1998).

In previous work (Lash et al., 2002a), we expressed recombinant rat DIC (rDIC) as the *N*-His_6-fusion protein from rat kidney in *E. coli*, reconstituted the purified DIC into proteoliposomes, and showed that it functions in transport of both dicarboxylates and GSH with properties similar to those of intact mitochondria. We then transiently transfected the cDNA for rDIC in a cell line derived from rat kidney proximal tubules (NRK-52E cells). The recombinant rDIC-His_6 in transfected NRK-52E cells localizes in mitochondria whereupon it mediates GSH uptake, thereby demonstrating function of the carrier in an intact renal cell. Furthermore, overexpression of the rDIC in NRK-52E cells markedly protected against apoptosis induced by either DCVC or *tert*-butyl hydroperoxide (tBH), supporting the toxicological significance of the mitochondrial GSH transport process.

In the present work, we studied the function of the rOGC, as both a bacterial expressed and reconstituted protein and in transfected NRK-52E cells. We then generated a double-cysteine mutant of the rOGC and showed that it exhibits markedly lower transport activity than the wild-type carrier. cDNAs for both the wild-type and double-cysteine mutant of the rOGC were then stably transfected into NRK-52E cells to assess further the influence of genetic manipulation of mitochondrial GSH transport activity on susceptibility of the cells to chemically induced apoptosis. Our results provide further evidence that manipulation of mitochondrial GSH transport activity in a renal cell line can modulate responses to cytotoxic chemicals.

Methods

Experimental design. The overall objective of this study was to determine whether modulation of mitochondrial concentrations of GSH can alter susceptibility of a renal proximal tubular cell to chemically induced apoptosis. Mitochondrial GSH status was altered by stable transfection of NRK-52E cells, a stable cell line derived from rat proximal tubules, with either the cDNA for rOGC or a double-cysteine mutant rOGC-C221,224S that exhibits markedly reduced transport function. Thus, comparisons were made between wild-type NRK-52E cells, which possess relatively low transport function and levels of mitochondrial GSH, NRK-52E cells stably overexpressing the rOGC, which possess high transport function and levels of mitochondrial GSH, and NRK-52E cells stably overexpressing the rOGC-C221,224S, which possess low to moderate transport function and moderate levels of mitochondrial GSH. Two well-characterized mitochondrial toxicants, tBH and DCVC, were used at concentrations that are known to cause apoptosis but little or no necrosis. Additionally, incubations were performed for relatively short time periods as this is also the time frame over which the cells primarily undergo apoptosis.

Materials. L-[^{3}H-glycyl]-GSH (44.8 Ci/mmol) and [^{14}C]-2-OG (281 mCi/mmol) were purchased from DuPont NEN (Boston, MA). Restriction enzymes for PCR, other enzymes (e.g., DNA polymerases, T7 RNA polymerase), and plasmids were purchased from New England Biolabs (Boston, MA), Promega (Madison, WI), and Gibco-BRL/Life Technologies (Gaithersburg, MD). PCR primers were custom synthesized by Integrated DNA Technology, Inc. (Coralville, IA). Cloning vectors (pGEM®-T Easy, pRSET, pcDNA3.1/V5-His-TOPO®) were purchased from Promega and Invitrogen (Carlsbad, CA). Dowex-1, Triton X-100, Percoll, phospholipids, and digitonin (aqueous type, recrystallized twice from hot ethanol) were purchased from Sigma (St. Louis, MO). Silicone oil (high temperature, n_D = 1.4950 at 20˚C, d = 1.050) and mineral oil (white, light, paraffin oil, n_D = 1.4760 at 20˚C, d = 0.862) were purchased from Aldrich Chemical (Milwaukee, WI). Materials for gel electrophoresis (SDS, acrylamide, agarose, buffers) were purchased from Bio-Rad (Richmond, CA) or Sigma. ProBond™ nickel-

JPET Fast Forward. Published on November 15, 2005 as DOI: 10.1124/jpet.105.094599
This article has not been copyedited and formatted. The final version may differ from this version.

chelating resin was purchased from Invitrogen. Millicell polycarbonate filter inserts (0.2 μm pore size, 25 mm diameter) were purchased from Millipore (Bedford, MA). NRK-52E cells (catalogue number CRL-1571) and cell culture medium (catalogue number 30-2002; Dulbecco's modified Eagle's medium with 4 mM L-glutamine adjusted to contain 1.5 g/l sodium bicarbonate, 4.5 g/l glucose, 1.0 mM sodium pyruvate), and 10% (w/v) bovine calf serum were purchased from the American Type Culture Collection (Manassas, VA). Antibodies to the His_6-fusion proteins were purchased from Invitrogen or Qiagen. DCVC was synthesized from trichloroethylene and L-cysteine in sodium metal and liquid ammonia (Elfarra et al., 1986). Purity (> 95%) was assessed by HPLC and TLC and identity was confirmed by ^{1}H-NMR. Double-distilled, deionized water was used for all experiments. All other chemicals and reagents were purchased from commercial vendors and were of the highest purity available.

Amplification of rat kidney mitochondrial rOGC cDNA by RT-PCR and bacterial expression. Total RNA was previously isolated from renal cortical homogenates of male Fischer 344 rats (200-300 g body weight; Charles River Laboratories, Wilmington, MA) by acid phenol extraction using the TRIZOL® extraction kit (Gibco-BRL/Life Technologies) and was stored at –80˚C until needed. Total rat kidney RNA was reverse transcribed with Superscript II reverse transcriptase and amplified with forward and reverse primers based on the complete cDNA sequence (1,149 bp) for the heart mitochondrial OGC protein from the Norway rat (*Rattus norvegicus*; sequence reported by Dolce et al. (1994); also see GenBank™ accession number NM_022398, which reports cDNA sequence corresponding to positions 42 to 987 of above sequence). PCR primers were designed with the aid of Oligo 6.7 (Molecular Biology Insights, Inc., Cascade, CO) based on the knowledge that the coding region is from positions 42 to 986, and were as follows: Upper primer = 5'–GCC GAG GGC CAT CAA GGG ACG ATT–3'; positions 21 to 43; lower primer = 5'–ACT TGG AAA CCC TGG CAC ACG AGT CTC A–3'; positions 1000 to 1027. RT-PCR was conducted by running 30 cycles of 94˚C x 3 min for denaturation and 70˚C x 2 min for annealing/extension. Sample was then loaded onto a 1% (w/v) agarose gel, the gel stained with ethidium bromide, and the bands visualized under UV light. The

1,149-bp product was ligated into a T-A cloning vector (pGEM®-T Easy) for transformation. Confirmation of the PCR product was by automated DNA sequencing.

The full-length cDNA for rat kidney OGC was subcloned into the pRSET T7 expression vector for high-level expression in *E. coli* as an *N*-terminal polyhistidine (His_6) fusion product. Bacterial cells containing the overexpressed protein were harvested by centrifugation (5,000*g* x 5 min at 4˚C), supernatants were discarded, and pellets were resuspended in 20 ml of TE-1 buffer (50 mM Tris-HCl, 2 mM EDTA, pH 8.0). Cells were then lysed by incubation for 15 min at 30˚C and occasional mixing with 100 µg of lysozyme/ml (freshly prepared in TE-1 buffer) and 0.1% (v/v) Triton X-100. Bacterial DNA in the cell lysate was sheared by sonication, the suspension centrifuged at 12,000*g* x 15 min, and the pellet resuspended in 2 ml of TE-2 buffer (10 mM Tris-HCl, 0.1 mM EDTA, 1 mM dithioerythritol, pH 7.0) and recentrifuged. The final pellet was resuspended in 2 ml of TE-2 buffer and was solubilized with 1.2% (w/v) sarkosyl dissolved in TE-2 buffer. The inclusion body fraction was isolated by centrifugation of the resuspended pellet at 131,000*g* x 4.5 hr through a step sucrose gradient [12.4 ml of 40% (w/v) sucrose and 18.6 ml of 53% (w/v) sucrose (sucrose solutions prepared in TE-2 buffer)]. The inclusion body pellet was resuspended in 30 ml of TE-2 buffer and centrifuged at 12,000*g* x 15 min. The OGC protein was then extracted by resuspension of the inclusion body pellet in 2 ml of 1.2% (w/v) sarkosyl dissolved in TE-2 buffer and centrifugation at 314,000*g* x 30 min.

Purity of the rOGC-His_6 fusion protein obtained from the inclusion body fraction was enhanced by fractionation of the inclusion body pellet (2 ml, approx. 25 mg protein) on a 1.0 x 6.8 cm column with 4 ml of nickel-chelating resin and equilibrated with ProBond™ buffer (20 mM potassium phosphate, pH 7.8, containing 500 mM NaCl). The column was then washed with ProBond™ buffer adjusted to pH 6.0 (25 ml) and finally with 25-ml each of ProBond™ buffer, pH 6.0, containing 100 mM and then 300 mM imidazole.

Preparation of proteoliposomes for reconstitution of purified rOGC. Liposomes and proteoliposomes were prepared essentially as described previously (Chen et al., 2000). Briefly, liposomes were prepared by transferring 700 mg of phosphatidylcholine into a 30-ml

JPET Fast Forward. Published on November 15, 2005 as DOI: 10.1124/jpet.105.094599
This article has not been copyedited and formatted. The final version may differ from this version.

polypropylene tube and drying under a stream of nitrogen. After redissolving the dried lipid in diethyl ether and removal of solvent under nitrogen, liposome buffer (7 ml; 120 mM HEPES, 50 mM KCl, 1 mM EDTA, pH 7.0) was added to the dried lipid, the tube was flushed with nitrogen, sealed, and vigorously mixed on a vortex mixer. Lipid was then dispersed in a bath sonicator for approximately 60 min and was stored at –80˚C for up to 3 months. Proteoliposomes were prepared by mixing purified carrier protein (200 µl, 50 µg protein) or liposome buffer (for a blank control) with 0.5 ml of liposomes and 50 µl of substrate solution (buffer containing 20 mM 2-OG) in a final volume of 1 ml. After mixing on a vortex mixer, the proteoliposomes were rapidly frozen in liquid nitrogen and stored at –80˚C for up to 1 month until use. Immediately prior to assay, the proteoliposome suspension was thawed, sonicated with a bath sonicator at room temperature, placed on ice for 1 min, and then passed through an anion exchange column (Dowex-1, 100-200 mesh, equilibrated with liposome buffer and prepared in a 9-inch Pasteur pipette) to remove external substrate by elution with liposome buffer. The opalescent fraction (approximately 1 ml) containing the proteoliposomes was collected. The proteoliposomes were equilibrated at room temperature for approximately 5 min before being used in transport assays. This freeze-thaw cycle and sonication method gives rise to a heterogeneous population of large, primarily unilamellar proteoliposomes that are suitable for transport studies (Kaplan and Pedersen, 1985).

Transport assays in reconstituted proteoliposomes. Transport of substrates (i.e., GSH, 2-OG) into proteoliposomes was measured by first preincubating 200 µl of proteoliposomes (preloaded with 1 mM 2-OG) for 1 min with 12 µl of ‘Reconstitution Buffer’ (120 mM HEPES, 50 mM KCl, 1 mM EDTA, pH 7.4). Competitive inhibitors were added simultaneously with substrates. Transport was initiated by addition of 12 µl of 20X radiolabeled substrate. At various times (30 to 240 sec), 30 µl aliquots were transferred to a microcentrifuge tube containing 70 µl of “Reconstitution Buffer’ + 40 mM of an irreversible transport inhibitor (i.e., pyridoxal 5’-phosphate), tubes were mixed and were placed on ice until the next processing step. After completion of time courses, samples were loaded onto Sephacryl S-100 mini-columns, which

JPET Fast Forward. Published on November 15, 2005 as DOI: 10.1124/jpet.105.094599
This article has not been copyedited and formatted. The final version may differ from this version.

were prepared in 5.75-inch Pasteur pipettes. These columns were placed in 16 x 125 mm glass test tubes and were centrifuged at 2,300 rpm x 2 min in a tabletop clinical centrifuge. Supernatant from each tube was transferred to a 5-ml scintillation vial, each tube was washed with 200 µl of scintillation fluid, which was then added to scintillation vials.

Uptake rates were calculated by linear curve-fitting as described previously (Chen and Lash, 1998; Chen et al., 2000), plotting $\ln[P_{total}/(P_{total} - P_t)]$ vs. time according to Halestrap (1975). P_{total} represents the total uptake of substrate at equilibrium (estimated by exponential decay curve-fitting of time course data) and P_t represents substrate uptake at time t (0 to 5 min). The initial rates of uptake were then determined from the first-order rate equation $v = k (P_{total})$.

As a control, liposomes were reconstituted with either buffer and no protein or protein that was inactivated by boiling for 5 min. These control liposomes exhibited less than 5% of the measured uptake of either GSH or 2-OG (data not shown), similar to previous reconstitution studies (Chen et al., 2000), indicating that nearly all of the measured substrate transport was due to the function of the reconstituted carrier protein.

Site-directed mutagenesis for generation of a double-cysteine mutant of rOGC. A double-cysteine mutant of the rOGC (rOGC-C221,224S), in which C221 and C224 were converted to S, was generated by nested PCR using two sets of upstream and downstream primers: Upstream primer 1 = 5'–GCC GAG GGC CAT CAA GGG ACG AT–3'; downstream primer 1 = 5'–GCG GAG AAG TGG GAC AGA ATG TTG TCA G–3'; upstream primer 2 = 5'–ATT CTG TCC CAC TTC TCC GCC AGC ATG AT–3'; downstream primer 2 = 5'–GAC TTG GAA ACC CTG GCA CAC GAG TCT CA–3'. The double-cysteine mutant, rOGC-C221,224S, was expressed in *E. coli* as the *N*-His_6 fusion protein, purified from inclusion bodies and by Ni^{2+}-affinity chromatography, and reconstituted into proteoliposomes as described above for the wild-type rOGC.

Culture of NRK-52E cells. NRK-52E cells were cultured on collagen-coated, polystyrene T-25 or T-175 culture flasks with Dulbecco's modified Eagle's medium containing 4% (w/v) glutamine, 1.5 g/l sodium bicarbonate, 4.5 g glucose/l, 1 mM sodium pyruvate, and

10% (v/v) bovine calf serum in an atmosphere of 5% CO_2, 95% air at 37˚C. On reaching confluence (5 to 9 days), subcultures were prepared by a 15-min treatment with 0.02% (w/v) EDTA, 0.05% (w/v) trypsin solution and replating the cells at a density of 4 x 10^4 cells/cm^2.

Transfection of NRK-52E cells. Plasmid DNA was purified, following amplification in *E. coli* cells, using the Promega Wizard Prep purification kit. cDNAs for either wild-type rOGC or rOGC-C221,224S were subcloned into the pcDNA3.1/V5-His-TOPO® vector and stably transfected into the NRK-52E cells with FuGene 6 from Roche Applied Science (Indianapolis, IN). Transfections were carried out as described by the manufacturer using a 3:1 ratio of FuGene 6 reagent to plasmid DNA. After 24 hr, cells were harvested by incubating with Cellstripper™ (Mediatech, Herndon, VA) for 5 min and gentle scraping. Stable transfectants were selected with G418.

Isolation of mitochondria from NRK-52E cells and transport measurements. Mitochondria were prepared from 7 confluent T-175 flasks, which contain approximately 70 to 85 x 10^6 NRK-52E cells, by differential centrifugation as described previously (McKernan et al., 1991). Yields of mitochondrial protein ranged from 6 to 10.5 mg. Purity of mitochondria was determined by measurement of activities of marker enzymes for mitochondria (succinate dehydrogenase, glutamate dehydrogenase), plasma membrane (alkaline phosphatase, (Na^++K^+)-stimulated ATPase), cytoplasm (lactate dehydrogenase), and endoplasmic reticulum (glucose 6-phosphatase) in whole cells and the mitochondrial fraction (Lash et al., 2002b). Most of the total cellular activity of the mitochondrial marker enzymes (≥ 75%) was recovered in the mitochondrial fraction whereas minimal to modest amounts of total cellular activity of markers for the other subcellular organelles were recovered in this fraction. Specifically, approximately 5% of total cellular activity of markers for the plasma membrane and endoplasmic reticulum and < 2% of total activity of the cytoplasmic marker enzyme were recovered in the mitochondrial fraction. This indicates that the mitochondrial fraction obtained from the NRK-52E cells is of high purity and has minimal contamination with other subcellular organelles.

For transport measurements, mitochondria were suspended in 3 ml of sucrose-triethanolamine buffer in 25-ml Erlenmeyer flasks. Radiolabeled 2-OG (1 mM final concentration, containing 0.8 µCi; 147 cpm/nmol) or GSH (5 mM final concentration, containing 0.8 µCi; 23.4 cpm/nmol) was added to initiate transport. Aliquots (0.5 ml) were removed at 1, 2, 5, and 10 min and were added to 1.5-ml microcentrifuge tubes, which were centrifuged at 13,000*g* x 30 sec. The mitochondrial pellets were washed twice with buffer, suspended in 0.5 ml of buffer, and transferred to a scintillation vial and radioactivity determined. No differences were observed if measurements were performed in mitochondria treated with antimycin A to inhibit metabolism, as previously found (Chen and Lash, 1998).

SDS PAGE and Western blotting. For gel electrophoresis, 10 or 20 µg of protein was loaded per well onto a 10% (w/v) or a 12% (w/v) polyacrylamide gel (Bio-Rad, Hercules, CA), and separation was achieved according to the method of Laemmli (1970). Total protein was visualized by staining with Coomassie Brilliant Blue G. For Western blot analysis, protein was transferred by electroblotting to a nitrocellulose membrane (MSI, Westborough, MA), blocked with 3% (w/v) bovine serum albumin (Promega, Madison, WI), washed with Tris-buffered saline containing Tween 20 (TTBS), probed with a monoclonal anti-RGSHHHH tag antibody (Qiagen, Valencia, CA), washed with TTBS, and then probed with an anti-mouse IgG antibody conjugated to alkaline phosphatase (Jackson Immunoresearch, West Grove, PA). Immunoreactive bands were visualized following incubation with a solution containing 5-bromo-4-chloro-3-indolyl-phosphate/nitro blue tetrazolium (Promega).

Digitonin fractionation of NRK-52E cells and analysis of mitochondrial contents of substrates. To analyze distribution of transported substrates into mitochondria of NRK-52E cells, subcellular fractions were separated by digitonin fractionation (Lash et al., 1998). Briefly, microcentrifuge tubes (1.5-ml capacity) were layered from the bottom with 0.25 ml of 40% (v/v) glycerol, 0.5 ml of silicone oil:paraffin oil (6:1), and 0.1 ml of 2-(*N*-morpholino)ethane sulfonic acid (Mes) buffer (19.8 mM Mes, pH 7.4, containing 19.8 mM EGTA, 19.8 mM EDTA, and 0.25 M mannitol) ± 0.15 mg digitonin. To fractionate cells, 0.5-ml aliquots of cells were mixed

JPET Fast Forward. Published on November 15, 2005 as DOI: 10.1124/jpet.105.094599
This article has not been copyedited and formatted. The final version may differ from this version.

with the top layer and microcentrifuge tubes were centrifuged at 13,000*g* x 3 min. In the absence of digitonin, the supernatant = extracellular medium and the pellet = total cellular contents. In the presence of digitonin, the supernatant = extracellular medium + cytoplasm and the pellet = mitochondrial fraction.

Flow cytometry analysis of cell cycle and quantitation of apoptosis. Cell cultures were washed twice with sample buffer (PBS plus 1 g glucose/l filtered through a 0.22-µm filter), dislodged by trypsin/EDTA incubation, centrifuged at 400*g* x 10 min at 22˚C, and resuspended in sample buffer. Cell concentrations were adjusted to 1 to 3 x 10^6 cells/ml with sample buffer and 1 ml of the cell suspension was centrifuged at 400*g* x 10 min at 22˚C. All of the supernatant except 0.1 ml/10^6 cells was removed and the remaining cells were mixed on a vortex mixer in the remaining fluid for 10 sec. Next, 1 ml of ice-cold ethanol (70%, v/v) was added to the sample in a dropwise manner, with samples being mixed for 10 sec between drops. Tubes were capped and fixed in ethanol at 4˚C. After fixation, cells were stained with propidium iodide (50 µg/ml) containing RNase A (100 U/ml). Samples were then mixed, centrifuged at 1,000*g* x 5 min at 22˚C and all the ethanol except 0.1 ml was removed. Cells were mixed in the residual ethanol and 1 ml of the propidium iodide staining solution was added to each tube. After mixing again, cells were incubated at room temperature for at least 30 min. Samples were analyzed within 24 hr by flow cytometry using a Becton Dickinson FACS*Calibur* Flow Cytometer, which is a core facility of the NIEHS Center for Molecular Toxicology with Human Applications at Wayne State University. Analyses were performed with 20,000 events per sample using the ModFit LT v. 2 for Macintosh data acquisition software package (Verity Software House, Inc., Topsham, ME; distributed by Becton Dickinson Immunocytochemistry System BDIS, San Jose, CA). Propidium iodide was detected by the FL-2 photomultiplier tube. Fractions of apoptotic cells were quantified by analysis of the sub-G_1 (sub-diploid) peak with ModFit cell cycle analysis. The percent distribution of cells in the various stages of the cell cycle (G_0/G_1, S, G_2/M) were also calculated. Cell aggregates were discarded in the flow cytometry analysis by post-fixation aggregate discrimination.

Data analysis. Data were normalized to protein content, which was determined by the bicinchoninic acid (BCA) protein assay from Pierce. All measurements were performed 3 to 5 times. Significant differences between means were first assessed by a one-way or two-way analysis of variance, depending on the comparisons being tested. When significant "F-values" were obtained, the Fisher's protected least significant difference t-test was performed to determine which means were significantly different from one another, using a two-tail probability, $P < 0.05$, as the criteria for significance.

Results

Tissue-specific variations in rOGC cDNA and amino acid sequences. In the course of amplifying the cDNA of mitochondrial OGC using total rat kidney RNA as a template, we discovered that the sequence of our PCR products exhibited significant differences from the rat heart and brain mitochondrial OGC cDNAs, which are the only two rat tissues from which the mitochondrial OGC cDNA sequence is available in either the literature or in GenBank™ **(Table 1)**. The PCR reaction was performed on 10 separate occasions, each time with the identical sequence being obtained for the product. Nucleotide differences were observed for 6 bp between kidney and heart and for 10 bp between kidney and brain. Amino acid differences for deduced sequences include 2 residues between kidney and heart and 6 residues between kidney and brain. While neither of the 2 amino acid differences between kidney and heart OGC are in predicted transmembrane domains (TMDs) and both are substitutions of amino acids that are similar in terms of charge and polarity (T for A and T for I), 2 of the amino acid differences between kidney and brain OGC are in predicted TMDs (TMD2 and TMD3) and one difference is very close to TMD1. Two of these differences are substitutions of amino acids that differ by charge or polarity (K for N and T for P) and, therefore, could have a significant effect on protein tertiary structure.

There is also uncertainty about the identity of transporters for 2-OG and GSH in rat liver. Although rat liver OGC may have a high degree of homology with rat brain OGC (Coll et al., 2003), its sequence has not been reported. While many of the reported properties of GSH and 2-OG transport in rat liver mitochondria are similar to what we have found in rat kidney mitochondria (Coll et al., 2003), GSH transport in rat liver mitochondria was inhibited by L-glutamate, which differs from our previous findings. A thorough search of the GenBank™ database and the published literature, however, failed to find any cDNA or amino acid sequences for the OGC from rat liver mitochondria. Fiermonte et al. (2001), however, reported cloning and expression of a rat liver oxodicarboxylate carrier (ODC) that transports 2-OG and other C5-C7

JPET Fast Forward. Published on November 15, 2005 as DOI: 10.1124/jpet.105.094599
This article has not been copyedited and formatted. The final version may differ from this version.

dicarboxylates. They isolated a 1456-bp cDNA with a 99-bp 5'-untranslated region, an open reading frame of 897 bp, and a 460-bp 3'-untranslated region. The cDNA encodes a polypeptide of 298 amino acids with a molecular mass of 33,276, which contrasts with the OGC from rat kidney, heart, and brain mitochondria, which are all 314 amino acids in length.

Bacterial expression of the rOGC and rOGC-C221,224S. The OGC contains three cysteinyl residues (C184, C221, C224), with the latter two being linked in a disulfide bond in the native protein (Palmieri et al., 1996). Considering that the two latter cysteinyl residues are conserved across species (for the limited number of species for which the cDNA and deduced amino acid sequences are published), are in TMD3, and that alteration of disulfide bridges should alter protein structure and function, we mutated both cysteinyl residues to serines and investigated effects on transport function and the ability of NRK-52E cells transfected with the cDNA for the double-cysteine mutant to be protected from toxicant-induced apoptosis.

The full-length cDNAs for wild-type (WT) rOGC and the double-cysteine mutant rOGC-C221,224S were expressed in *E. coli* as *N*-His_6 fusion proteins and purified from inclusion bodies followed by Ni^{2+}-affinity chromatography. Analysis by Coomassie staining of SDS gels for presence of rOGC-His_6 **(Fig. 1A)** or rOGC-C221,224S-His_6 **(Fig. 1B)** showed that a substantial degree of purification was achieved by passing the solubilized material from the inclusion body fraction through the Ni^{2+}-affinity column (compare lane 1 with lanes 5-7 in Fig. 1A and lane 1 with lanes 6-9 in Fig. 1B). IPTG-stimulated, time-dependent increases in protein expression, as shown by Western blot analysis using the monoclonal anti-RGSHHHH tag antibody, with the expected molecular weight of 34-37 kDa were observed for both the WT **(Fig. 1C)** and double-cysteine mutant **(Fig. 1D)** carriers. The overall yield of both the WT and double-cysteine mutant proteins from a one-liter culture of bacteria was typically 20 to 25 mg of protein.

Reconstitution and transport function of rOGC and rOGC-C221,224S. The bacterial expressed and purified rOGC was reconstituted in proteoliposomes for assessment of its ability to transport 2-OG and GSH. Similar to results with the partially purified and reconstituted inner membrane transporter preparation (Chen et al., 2000), the expressed and reconstituted rOGC

JPET Fast Forward. Published on November 15, 2005 as DOI: 10.1124/jpet.105.094599
This article has not been copyedited and formatted. The final version may differ from this version.

exhibited time- and concentration-dependent uptake of both 2-OG **(Fig. 2A)** and GSH **(Fig. 2B)** with maximal accumulation of substrate after 2- to 3-min of incubation, followed by a decrease at later time points. This spike is consistent with heteroexchange of *trans*- for *cis*-substrate. As two controls, liposomes were either reconstituted without added purified protein and uptake of substrates was measured or protein was boiled prior to incorporation into proteoliposomes and measurement of uptake. As found in previous studies of ours (Chen et al., 2000; Lash et al., 2002a), both controls exhibited < 5% of the apparent uptake of radiolabeled 2-OG or GSH, indicating that transport in the proteoliposomes is due to a catalytically active protein (data not shown).

Initial rates of uptake were derived as described in *Materials and Methods* and Eadie-Hofstee plots were constructed to derive kinetic parameters **(Table 2)**. The results show that 2-OG is a much better substrate for the rOGC than is GSH, with the carrier having a 6.9-fold lower K_m value for 2-OG than for GSH, although the K_m for GSH is well within the range of normal concentrations of GSH in proximal tubular cytoplasm. V_{max} values for 2-OG or GSH as substrates were similar.

Bacterial expressed, purified, and reconstituted rOGC-C221,224S likewise exhibited time- and concentration-dependent uptake of both 2-OG **(Fig. 3A)** and GSH **(Fig. 3B)**. Similar to transport function for the rOGC-WT, intravesicular accumulation of either substrate exhibited maximal values at approximately 2 min, with modest decreases thereafter. Analysis of kinetic parameters for each substrate by Eadie-Hofstee plots using calculated initial rates **(Table 2)** showed that the double-cysteine mutant carrier exhibited a 70% and 81% decrease in V_{max} for 2-OG and GSH, respectively, and a 13.6-fold and 14.4% increase in K_m for 2-OG and GSH, respectively. In spite of the modest effect on the K_m value for GSH, it is clear that the transport function of the double-cysteine mutant is markedly diminished as compared to that of the wild-type carrier.

Transport activity of both the rOGC-WT and rOGC-C221,224S with either 2-OG or GSH as substrate was markedly (> 80%) inhibited by either PLP or phenylsuccinate (PhSucc) **(Figs. 4 and 5)**, which is consistent with the expected sensitivity of the carrier.

Effect of stable transfection of NRK-52E cells with cDNAs for rOGC-WT and rOGC-C221,224S on susceptibility to chemically induced apoptosis. NRK-52E cells were stably transfected with either the cDNA for rOGC-WT or rOGC-C221,224S by selection with G418. Expression of the rOGC-WT protein **(Fig. 6A)** and the rOGC-C221,224S protein **(Fig. 6B)** in mitochondrial extracts from stably transfected NRK-52E cells was confirmed by Western blot analyses using the monoclonal anti-RGSHHHH tag antibody.

Before determining the influence of expression of either wild-type or mutant rOGC in the NRK-52E cells on susceptibility to chemically induced apoptosis, we compared the ability of mitochondria from the three cell populations (i.e., non-transfected cells – NRK-52E-WT; cells transfected to overexpress rOGC – NRK-52E-rOGC; cells transfected to overexpress the double-cysteine mutant carrier – NRK-52E-rOGC-C221,224S) to accumulate either GSH (**Fig. 7)** or 2-OG **(Fig. 8)**. Each population of NRK-52E cells was incubated with the indicated concentrations of either substrate for various times up to 60 min, and cell samples were washed and fractionated by digitonin treatment to separate cytoplasmic and mitochondrial compartments. Results shown for 30-min incubations indicate that cells overexpressing rOGC exhibited markedly higher contents of GSH in mitochondria than either NRK-52E-WT or NRK-52E-rOGC-C221,224S cells, with the latter cell population exhibiting the lowest content of GSH in mitochondria **(Fig. 7A)**. The increase in contents of mitochondrial GSH were prevented by including the rOGC inhibitor PhSucc **(Fig. 7B)**, demonstrating that the alterations in mitochondrial contents of GSH were due to rOGC. Concentrations of GSH in the cytoplasm of the three populations of NRK-52E cells incubated with exogenous GSH were also measured (data not shown). While differences between the three cell populations were observed, these were smaller than those for mitochondrial GSH contents and exhibited an inverse pattern among the three cell populations as compared to the pattern for mitochondria. Thus, the highest GSH concentrations in cytoplasm

were observed in NRK-52E-WT cells whereas the lowest GSH concentrations in cytoplasm were observed in NRK-52E-rOGC cells and the NRK-52E cells overexpressing the double-cysteine mutant exhibited intermediate levels of GSH in the cytoplasm.

Similar incubations using 2-OG as transporter substrate also demonstrated markedly increased mitochondrial contents of 2-OG in NRK-52E-rOGC cells as compared with either non-transfectants or cells expressing the double-cysteine mutant **(Fig. 8A**). Co-incubation with 10 mM PhSucc also markedly diminished most of the increased contents of mitochondrial 2-OG **(Fig. 8B)**, indicating that the altered mitochondrial contents of 2-OG were largely due to the different levels of activity of the OGC.

The three populations of NRK-52E cells were then incubated for 1, 2, or 4 hr with either media (= Control), 10 or 50 µM tBH, or 50 or 200 µM DCVC for assessment of the fraction of cells undergoing apoptosis **(Fig. 9)**. While all three populations of control cells exhibited < 1.5% apoptosis throughout the 4-hr time course, NRK-52E-WT cells exhibited dose-dependent increases in the fraction of cells undergoing apoptosis after exposure to either tBH or DCVC at all time points, with increases from 1- to 2-hr incubations and slightly less apoptosis after 4-hr incubations **(Fig. 9A-C)**. This decrease by the 4-hr time point is likely due to cells losing competence to undergo apoptosis and switching to necrosis as a mode of cell death (see also Lash et al., 2002a, 2002b). NRK-52E-rOGC cells, in contrast, exhibited very small increases in apoptosis after toxicant exposures, indicating significant protection **(Fig. 9D-F)**. NRK-52E-rOGC-C221,224S cells, however, exhibited comparable amounts of apoptosis as NRK-52E-WT cells. Maximal amounts of apoptotic cells (12 to 13%) were observed with NRK-52E-rOGC-C221,224S cells incubated for 2 hr with either 50 µM tBH or 200 µM DCVC **(Fig. 9G-I)**.

JPET Fast Forward. Published on November 15, 2005 as DOI: 10.1124/jpet.105.094599
This article has not been copyedited and formatted. The final version may differ from this version.

Discussion

The present study sought to further define the role of mitochondrial GSH transporters in determining the susceptibility of renal proximal tubular cells to chemically induced apoptosis, focusing on the OGC and using NRK-52E cells as a model system. NRK-52E cells are an excellent model in which to examine these processes because they exhibit many properties of *in vivo* proximal tubules, including retention of epithelial morphology and expression of high activities of the (Na^+ + K^+)-ATPase and several enzymes of the GSH redox cycle (Lash et al., 2002b). Unlike the *in vivo* proximal tubule and similar to other epithelial-derived, immortalized cell lines, NRK-52E cells exhibit relatively low activities of brush-border membrane enzymes and relatively low activities of mitochondrial respiration, transport, and dehydrogenase enzymes (Lash et al., 2002b). Whereas mitochondrial GSH content represents approximately 30% of the total cellular pool of GSH in the *in vivo* rat proximal tubule (Lash et al., 1998; Schnellmann et al., 1988), it comprises only 8-10% of the total cellular GSH pool in NRK-52E cells. In spite of this, the relatively high activity of the (Na^+ + K^+)-ATPase argues that cellular supplies of ATP, and hence mitochondrial function, are adequate for cellular work under normal, physiological conditions. These differences between NRK-52E cells and the *in vivo* proximal tubule actually facilitate our transport measurements because they provide a model that has low activity of GSH degradation and a low baseline level of mitochondrial transport activity. Although it can be argued that the NRK-52E cells are inherently more sensitive than the *in vivo* rat proximal tubule to toxicants because of their lower mitochondrial GSH content, the ability to modulate mitochondrial GSH contents over a wide range of values, that include those that greatly exceed those in the *in vivo* proximal tubule, allows us to directly test the hypotheses we have posed.

After amplification of the cDNA for the rOGC using total rat kidney cortex RNA as a template, comparison of the kidney rOGC DNA sequence with those of the rOGC from rat heart and brain showed differences between these published sequences and that for our PCR product from rat kidney. Moreover, comparison of the deduced amino acid sequences from the rat kidney

JPET Fast Forward. Published on November 15, 2005 as DOI: 10.1124/jpet.105.094599
This article has not been copyedited and formatted. The final version may differ from this version.

PCR product with that from rat heart and brain showed two and six amino acid residue differences, respectively, two of which between our rat kidney product and that from rat brain differed by polarity or charge. Because these two differences are in TMDs and likely lead to changes in protein three-dimensional structure, catalytic function of the rOGC from rat kidney and brain may differ. This suggests that tissue-specific differences may exist in the rOGC.

Although the cDNA sequence for rat liver OGC is not published in GenBank™, Coll et al. (2003) used the cDNA sequence from rat brain OGC to design primers to detect expression of the OGC in rat liver. From this, one would conclude that the cDNA sequence for rat liver OGC is very similar to or the same as that from rat brain. To complicate matters, however, Fiermonte et al. (2001) identified a carrier, called the ODC, that transports 2-OG but exhibits no significant cDNA sequence homology and only 25-27% amino acid homology with the deduced amino acid sequences of our cDNA clone or the two published sequences of rOGC from heart or brain. Repetition of the PCR reaction 10 times, with confirmation by sequencing the PCR cDNA product and expression, purification, and functional reconstitution of the OGC protein, provide confidence that the sequence differences among tissues are real and not due to PCR artifacts. Although additional work is required to clarify the identity and function of carriers for 2-OG and GSH in rat liver, the possibility that the cDNA and deduced amino acid sequences of our OGC cDNA from rat kidney differ significantly from those of other tissues warrants further study.

Transport properties of the amplified, bacterial expressed, and reconstituted rOGC from kidney were consistent with the function of this carrier that we observed previously in suspensions of rat kidney mitochondria (Chen and Lash, 1998) and proteoliposomes reconstituted with a partially purified preparation of mitochondrial inner membrane carriers from rabbit kidney mitoplasts (Chen et al., 2000). These similarities included a lower K_m but a higher V_{max} for 2-OG than for GSH as transport substrate and inhibition of transport by PLP and PhSucc.

In a previous study (Lash et al., 2002a), we demonstrated that transient overexpression of the cDNA for the rDIC in NRK-52E cells produced a 3- to 11-fold increase in mitochondrial

GSH content and protected the cells from tBH- and DCVC-induced apoptosis. Because our previous work (Chen and Lash, 1998) concluded that the rDIC and rOGC contributed approximately 60% and 40%, respectively, to the uptake of GSH from cytoplasm into mitochondrial matrix, our expectation was that overexpression of the rOGC in NRK-52E cells would also provide significant protection from tBH- and DCVC-induced apoptosis. Indeed, this expectation was realized as stably transfected NRK-52E cells that overexpressed the rOGC were almost completely protected and significantly protected, respectively, from tBH- and DCVC-induced apoptosis. The difference in the ability to protect from tBH and DCVC likely lies in the distinct mechanisms of action of the two toxicants. Whereas tBH can be described as a “pure” oxidant that causes lipid peroxidation and GSH oxidation in mitochondria (McKernan et al., 1991), DCVC exerts mitochondrial toxicity by at least two mechanisms, including both an oxidative stress with increased lipid peroxidation and GSH oxidation (Lash and Anders, 1987), and inhibition of mitochondrial dehydrogenases by alkylation (Cooper et al., 2002; Hayden and Stevens, 1990; Lash and Anders, 1987; van de Water et al., 1995). The NRK-52E-rOGC cells also exhibited markedly higher contents of mitochondrial GSH than NRK-52E-WT cells when each population was incubated with exogenous GSH (cf. Fig. 7), indicating that the protection was associated with an enhanced ability of the transfectants to accumulate GSH in their mitochondria.

Although most prior studies of tBH- and DCVC-induced cellular injury have focused on the association of their biochemical effects with cellular necrosis, this occurs at much higher doses of toxicants than were used in the present study. Thus, while both tBH and DCVC can cause oxidation of mitochondrial GSH and cellular necrosis (Lash and Anders, 1987; Lash et al., 1998; McKernan et al., 1991), these same toxicants can result in apoptosis under appropriate exposure conditions (Lash et al., 2001). The pronounced oxidation of the mitochondrial GSH pool and lipid peroxidation previously described occurred at much higher concentrations than those used in the present study.

To explore how much mitochondrial GSH is necessary and sufficient to protect NRK-52E cells, we constructed a double-cysteine mutant of the renal rOGC by site-directed mutagenesis. While amplified, bacterial expressed, and reconstituted rOGC-C221,224S exhibited similar sensitivity to PLP and PhSucc as the wild-type carrier, it exhibited markedly lower catalytic efficiency (i.e., V_{max}/K_m values) for transport of 2-OG and GSH. NRK-52E-rOGC-C221,224S cells were no less sensitive than NRK-52E-WT cells to tBH- and DCVC-induced apoptosis. This lack of protection suggests that there is a threshold in the mitochondrial content of GSH that is needed to prevent cell death from oxidants or other mitochondrial toxicants. Consistent with this conclusion, mitochondrial accumulation of GSH was modestly lower in NRK-52E-rOGC-C221,224S cells than in NRK-52E-WT cells (cf. Fig. 7). This conclusion is also consistent with observations that certain forms of chemically induced cytotoxicity, notably oxidative stress, are dependent on depletion of mitochondrial GSH below a certain level (Fernandez-Checa et al., 1997; Martensson and Meister, 1989; Reed, 1990; Shan et al., 1993). Comparison of the extent of protection by overexpression of the rOGC over time, which was greater in the 1-hr and 2-hr incubations than in the 4-hr incubation, suggests that enhancing mitochondrial GSH content delays the progress of cellular injury.

In summary, the present studies have provided additional evidence that manipulation of mitochondrial GSH transport function can modulate renal cellular susceptibility to toxicants and have provided insight into the limitations of GSH levels required to elicit protection, consistent with the existence of a threshold level of mitochondrial GSH that is required for protection. Determination of this threshold concentration will require a more systematic analysis of correlations between transport rates, mitochondrial GSH content, and cellular susceptibility. The reported association of depletion or oxidation of hepatic mitochondrial GSH with several disease states, including chronic alcohol consumption and alcoholic liver disease (Fernandez-Checa et al., 1993) and cirrhosis and other forms of biliary obstruction (Krahenbuhl et al., 1992, 1995), emphasizes the importance of understanding how mitochondrial GSH is regulated. In the kidneys, studies have not directly addressed the question of mitochondrial GSH and disease,

although diabetic nephropathy is associated with oxidative stress and GSH oxidation (Obrosova et al., 2003). The potential clinical significance of modulating mitochondrial GSH content is further highlighted by a study using mouse B16 melanoma cells, in which the authors proposed that maintenance of mitochondrial GSH homeostasis may be required for survival of metastatic cells (Ortega et al., 2003). Hence, additional understanding of the regulation of mitochondrial GSH status and modulation of GSH levels holds promise for development of novel therapeutic approaches for many diseases and chemically induced toxicities.

References

Beatrice MC, Stiers DL and Pfeiffer DR (1984) The role of glutathione in the retention of Ca^{2+} by liver mitochondria. *J Biol Chem* 259:1279-1287.

Bisaccia F, Indiveri C and Palmieri F (1985) Purification of reconstitutively active α-oxoglutarate carrier from pig heart mitochondria. *Biochim Biophys Acta* 810:362-369.

Bisaccia F, Indiveri C and Palmieri F (1988) Purification and reconstitution of two anion carriers from rat liver mitochondria: the dicarboxylate and 2-oxoglutarate carrier. *Biochim Biophys Acta* 933:229-240.

Chen Z and Lash LH (1998) Evidence for mitochondrial uptake of glutathione by dicarboxylate and 2-oxoglutarate carriers. *J Pharmacol Exp Ther* 285:608-618.

Chen Z, Putt DA and Lash LH (2000) Enrichment and functional reconstitution of glutathione transport activity from rabbit kidney mitochondria: Further evidence for the role of the dicarboxylate and 2-oxoglutarate carriers in mitochondrial glutathione transport. *Arch Biochem Biophys* 373:193-202.

Coll O, Colell A, Garcia-Ruiz C, Kaplowitz N and Fernandez-Checa JC (2003) Sensitivity of the 2-oxoglutarate carrier to alcohol intake contributes to mitochondrial glutathione depletion. *Hepatology* 38:692-702.

Cooper AJL, Bruschi SA and Anders MW (2002) Toxic, halogenated cysteine S-conjugates and targeting of mitochondrial enzymes of energy metabolism. *Biochem Pharmacol* 64:553-564.

Dolce V, Messina A, Cambria A and Palmieri F (1994) Cloning and sequencing of the rat cDNA encoding the mitochondrial 2-oxoglutarate carrier protein. *DNA Sequence* 5:103-109.

Elfarra AA, Jakobson I and Anders MW (1986) Mechanism of S-(1,2-dichlorovinyl)glutathione-induced nephrotoxicity. *Biochem Pharmacol* 35:283-288.

Fernandez-Checa JC, Hirano T, Tsukamoto H and Kaplowitz N (1993) Mitochondrial glutathione depletion in alcoholic liver disease. *Alcohol* 10:469-475.

Fernandez-Checa JC, Kaplowitz N, Garcia-Ruiz C, Colell A, Miranda M, Mari M, Ardite E and Morales E (1997) GSH transport in mitochondria: Defense against TNF-induced oxidative stress and alcohol-induced defect. *Am J Physiol* 273:G7-G17.

Fiermonte G, Palmieri L, Dolce V, Lasorsa FM, Palmieri F, Runswick MJ and Walker JE (1998) The sequence, bacterial expression, and functional reconstitution of the rat mitochondrial dicarboxylate transporter cloned via distant homologs in Yeast and *Caenorhabditis elegans*. *J Biol Chem* 273:24754-24759.

Fiermonte G, Dolce V, Palmieri L, Ventura M, Runswick MJ, Palmieri F and Walker JE (2001) Identification of the human mitochondrial oxodicarboxylate carrier: Bacterial expression, reconstitution, functional characterization, tissue distribution, and chromosomal location. *J Biol Chem* 276:8225-8230.

Griffith OW and Meister A (1985) Origin and turnover of mitochondrial glutathione. *Proc Natl Acad Sci USA* 82:4668-4672.

Halestrap AP (1975) The mitochondrial pyruvate carrier: Kinetics and specificity for substrates and inhibitors. *Biochem J* 148:85-96.

Hayden PJ and Stevens JL (1990) Cysteine conjugate toxicity, metabolism, and binding to macromolecules in isolated rat kidney mitochondria. *Mol Pharmacol* 37:468-476.

Kakhniashvili D, Mayor JA, Gremse DA, Xu Y and Kaplan RS (1997) Identification of a novel gene encoding the yeast mitochondrial dicarboxylate transport protein via overexpression, purification, and characterization of its protein product. *J Biol Chem* 272:4516-4521.

Kaplan RS and Pedersen PL (1985) Isolation and reconstitution of the *n*-butylmalonate-sensitive dicarboxylate transporter from rat liver mitochondria. *J Biol Chem* 260:10293-10298.

Krahenbuhl S, Stucki J and Reichen J (1992) Reduced activity of the electron transport chain in liver mitochondria isolated from rats with secondary biliary cirrhosis. *Hepatology* 15:1160-1166.

Krahenbuhl S, Talos C, Lauterburg BH and Reichen J (1995) Reduced antioxidative capacity in liver mitochondria from bile duct ligated rats. *Hepatology* 22:607-612.

Kroemer G, Dallaporta B and Resche-Rigon M (1998) The mitochondrial death/life regulator in apoptosis and necrosis. *Annu Rev Physiol* 60:619-642.

Laemmli UK (1970) Cleavage of structural proteins during the assembly of the head of bacteriophage T4. *Nature* 227:680-685.

Lançar-Benba J, Foucher B and Saint-Macary M (1994) Purification of the rat-liver mitochondrial dicarboxylate carrier by affinity chromatography on immobilized malate dehydrogenase. *Biochim Biophys Acta* 1190:213-216.

Lash LH and Anders MW (1987) Mechanism of *S*-(1,2-dichlorovinyl)-L-cysteine- and *S*-(1,2-dichlorovinyl)-L-homocysteine-induced renal mitochondrial toxicity. *Mol Pharmacol* 32:549-556.

Lash LH, Visarius TM, Sall JM, Qian W and Tokarz JJ (1998) Cellular and subcellular heterogeneity of glutathione metabolism and transport in rat kidney cells. *Toxicology* 130:1-15.

Lash LH, Hueni SE and Putt DA (2001) Apoptosis, necrosis and cell proliferation induced by *S*-(1,2-dichlorovinyl)-L-cysteine in primary cultures of human proximal tubular cells. *Toxicol. Appl. Pharmacol.* 177:1-16.

Lash LH, Putt DA and Matherly LH (2002a) Protection of NRK-52E cells, a rat renal proximal tubular cell line, from chemical-induced apoptosis by overexpression of a mitochondrial glutathione transporter. *J Pharmacol Exp Ther* 303:476-486.

Lash LH, Putt DA, Hueni SE, Cao W, Xu F, Kulidjian SJ and Horwitz JP (2002b) Cellular energetics and glutathione status in NRK-52E cells: Toxicological implications. *Biochem Pharmacol* 64:1533-1546.

Lê-Quôc K and Lê-Quôc D (1985) Crucial role of sulfhydryl groups in the mitochondrial inner membrane structure. *J Biol Chem* 260:7422-7428.

Martensson J and Meister A (1989) Mitochondrial damage in muscle occurs after marked depletion of glutathione and is prevented by giving glutathione monoester. *Proc Natl Acad Sci USA* 86:471-475.

McKernan TM, Woods EB and Lash LH (1991) Uptake of glutathione by renal cortical mitochondria. *Arch Biochem Biophys* 288:653-663.

Obrosova IG, Fathallah L, Liu E and Nourooz-Zadeh J (2003) Early oxidative stress in the diabetic kidney: Effect of DL-α-lipoic acid. *Free Rad Biol Med* 34:186-195.

Ortega AL, Carretero J, Obrador E, Gambini J, Asensi M, Rodilla V and Estrela JM (2003) Tumor cytotoxicity by endothelial cells: Impairment of the mitochondrial system for glutathione uptake in mouse B16 melanoma cells that survive after *in vivo* interaction with the hepatic sinusoidal endothelium. *J Biol Chem* 278:13888-13897.

Palmieri F, Bisaccia F, Capobianco L, Dolce V, Fiermonte G, Iacobazzi V, Indiveri C and Palmieri L (1996) Mitochondrial metabolite transporters. *Biochim Biophys Acta* 1275:127-132.

Reed DJ (1990) Glutathione: Toxicological implications. *Annu Rev Pharmacol Toxicol* 30:603-631.

Schnellmann RG (1991) Renal mitochondrial glutathione transport. *Life Sci.* 49:393-398.

Schnellmann RG, Gilchrist SM and Mandel LJ (1988) Intracellular distribution and depletion of glutathione in rabbit renal proximal tubules. *Kidney Int* 34:229-233.

Shan X, Jones DP, Hashmi M and Anders MW (1993) Selective depletion of mitochondrial glutathione concentrations by (*R,S*)-3-hydroxy-4-pentenoate potentiates oxidative cell death. *Chem Res Toxicol* 6:75-81.

Smith CV, Jones DP, Guenther TM, Lash LH and Lauterburg BH (1996) Compartmentation of glutathione: Implications for the study of toxicity and disease. *Toxicol Appl Pharmacol* 140:1-12.

van de Water B, Zoeteweij JP, de Bont HJGM and Nagelkerke JF (1995) Inhibition of succinate:ubiquinone reductase and decrease of ubiquinol in nephrotoxic cysteine S-conjugate-induced oxidative cell injury. *Mol Pharmacol* 48:928-937.

Yagi T and Hatefi Y (1984) Thiols in oxidative phosphorylation: Inhibition and energy-potentiated uncoupling by monothiol and dithiol modifiers. *Biochemistry* 23:2449-2455.

Footnotes

This work was funded by National Institute of Diabetes and Digestive and Kidney Diseases Grant R01-DK40725 (to L.H.L. and L.H.M.).

Core facilities funded by the National Institute of Environmental Health Sciences Center for Molecular Toxicology with Human Applications (Grant P30-ES06639) at Wayne State University were used for some of these studies.

Address reprint requests to: Dr. Lawrence H. Lash, Department of Pharmacology, Wayne State University School of Medicine, 540 East Canfield Avenue, Detroit, MI 48201; Phone: (313)-577-0475; FAX: (313)-577-6739; E-mail: l.h.lash@wayne.edu.

Legends for Figures

Fig. 1. *Coomassie-stained SDS gels (A, B) and immunoblots (C, D) of wild-type (A, C)) and double-cysteine mutant (B, D) rOGC expressed in E.coli.*

Positive clones from BL21 Lys S cells were transformed with the pRSET B-OGC-WT (A, C) or pRSET C-OGC-C221,224S (B, D) cDNA inserts and were grown for 2 hr (panels A and B) or 0, 1, or 2 hr (panels C and D) in the presence of IPTG. Cells were then solubilized and put through several freeze-thaw cycles. Lysed cells were centrifuged at 10,000*g* X 5 min, and 20 µg protein was electrophoresed on 12% (w/v) polyacrylamide gels in the presence of SDS. *Panel A:* Lane 1: Flow-through from Ni^{2+}-affinity column; lane 2: Standards; lanes 3 and 4: Column wash; lanes 5-7: Column elution fractions. *Panel B:* Lane 1: *E. coli* extract; lane 2: Standards; lane 3: Flow-through from Ni^{2+}-affinity column; lanes 4 and 5: Column wash; lanes 6-8: Column elution fractions. Arrow = rOGC band. *Panels C and D:* Presence of either the OGC-WT-His_6 or OGC-C221,224S-His_6 fusion proteins in inclusion bodies were confirmed by Western blots using a monoclonal anti-RGSHHHH tag antibody with chemiluminescence detection. Expected products of MW 34-37 kDa were obtained.

Fig. 2. *Time and concentration dependence of 2-OG (A) and GSH (B) uptake by amplified, bacterial-expressed, and reconstituted rOGC-His_6.*

Uptake of [^{14}C]2-OG or [^{3}H]GSH was measured in proteoliposomes preloaded with 1 mM malate. At indicated times, aliquots of incubation mixtures were mixed with 40 mM PLP and centrifuged through Sephacryl S-100 mini-columns. Eluates were placed in scintillation vials for determination of radioactivity. Results are means ± SEM of measurements from 4 separate preparations.

Fig. 3. *Time and concentration dependence of 2-OG (A) and GSH (B) uptake by amplified, bacterial-expressed, and reconstituted rOGC-C221,224S-His$_{6.}$*

Uptake of [^{14}C]2-OG or [^{3}H]GSH was measured in proteoliposomes preloaded with 1 mM malate. At indicated times, aliquots of incubation mixtures were mixed with 40 mM PLP and centrifuged through Sephacryl S-100 mini-columns. Eluates were placed in scintillation vials for determination of radioactivity. Results are means ± SEM of measurements from 4 separate preparations.

Fig. 4. *Inhibition of 2-OG (A) and GSH (B) uptake in amplified, expressed, and reconstituted rOGC-His$_6$ by PLP and phenylsuccinate (PhSucc).*

Uptake of 1 mM [^{14}C]2-OG or [^{3}H]GSH was measured in proteoliposomes preloaded with 1 mM malate and in the presence of either substrate alone or with 40 mM PLP or 10 mM PhSucc. Samples were processed for determination of radioactivity as described in the legend to Figs. 2 and 3, and results are means ± SEM of measurements from 4 separate preparations.

Fig. 5. *Inhibition of 2-OG (A) and GSH (B) uptake in amplified, expressed, and reconstituted rOGC-C221,224S-His$_6$ by PLP and phenylsuccinate (PhSucc).*

Uptake of 1 mM [^{14}C]2-OG or [^{3}H]GSH was measured in proteoliposomes preloaded with 1 mM malate and in the presence of either substrate alone or with 40 mM PLP or 10 mM PhSucc. Samples were processed for determination of radioactivity as described in the legend to Figs. 2 and 3, and results are means ± SEM of measurements from 4 separate preparations.

Fig. 6. *Immunoblots of wild-type OGC (A) and OGC-C221,224S (B) from rat kidney mitochondria in NRK-52E cells.*

Mitochondria from three stable transfectants of NRK-52E cells expressing the wild-type OGC (A) or from two stable transfectants expressing the OGC-C221,224S mutant (B) were solubilized and put through several freeze-thaw cycles. Lysed mitochondria were centrifuged at 10,000g X 5 min, and 20 µg of protein was electrophoresed on a 12% (w/v) polyacrylamide gel in the presence of SDS. Presence of the OGC-His_6 or OGC-C221,224S-His_6 fusion proteins was confirmed by Western blots using the anti-His-C-terminal antibody with chemiluminescence detection. The expected product of MW 34-37 kDa was obtained.

Fig. 7. *GSH content in mitochondria of populations of NRK-52E cells transfected with either nothing (WT) or the cDNA for rOGC or rOGC-C221,224S.*

Each of the populations of NRK-52E cells were grown to confluence on T25 flasks and incubated with 1, 5, or 10 mM GSH containing 0.1 µCi L-[^{3}H-glycyl] GSH in the absence (A) or presence (B) of 10 mM PhSucc for 15, 30, or 60 min. Cells were removed from flasks and fractionated by digitonin treatment to quantify content of GSH in the mitochondrial fraction. Results are shown for 30-min incubations and are means ± SEM of measurements from 3-4 cell cultures. *Significantly different ($P < 0.05$) from the corresponding sample from WT cells.

Fig. 8. *2-OG content in mitochondria of populations of NRK-52E cells transfected with either nothing (WT) or the cDNA for rOGC or rOGC-C221,224S.*

Each of the populations of NRK-52E cells were grown to confluence on T25 flasks and incubated with 0.2, 0.5, or 1 mM 2-OG containing 0.1 µCi [^{14}C]-2-OG in the absence (A) or presence (B) of 10 mM PhSucc for 15, 30, or 60 min. Cells were removed from flasks and fractionated by digitonin treatment to quantify content of 2-OG in the mitochondrial fraction. Results are shown for 30-min incubations and are means ± SEM of measurements from 3-4 cell cultures. *Significantly different ($P < 0.05$) from the corresponding sample from WT cells.

Fig. 9. *Influence of modulation of mitochondrial GSH transport activity on susceptibility of NRK-52E cells to tBH- and DCVC-induced apoptosis.*

NRK-52E cells (either wild-type (WT; *Panels A-C*) or those stably transfected to overexpress either the normal cDNA for rOGC (rOGC; *Panels D-F*) or the double-mutant containing two Cysteine residues converted to Serines by RT-PCR (rOGC-C221,224S; *Panels G-I*) were preincubated for 24 hr with 1 mM GSH and then incubated for up to 4 hr with either medium (= Control), tBH (10 or 50 µM), or DCVC (50 or 200 µM). The fraction of cells undergoing apoptosis was estimated by propidium iodide staining and flow cytometry. Results are means ± SEM of 5 separate experiments for WT cells and 4 separate experiments for each of the transfectants. *Significantly different ($P < 0.05$) from the corresponding control sample. †Significantly different ($P < 0.05$) from WT cells incubated under the same conditions.

JPET Fast Forward. Published on November 15, 2005 as DOI: 10.1124/jpet.105.094599
This article has not been copyedited and formatted. The final version may differ from this version.

Table 1. *Tissue-specific differences in nucleotide and amino acid sequences of rat OGC.*

The published nucleotide and amino acid sequences from the heart, brain, and liver of the rat noted above are compared with those of the rat kidney that we obtained in our current study. Sequences were aligned using BLAST.

Tissue / Accession Numbers	**Nucleotide Sequences**	**Amino Acid Sequences**
vs. Heart OGC GenBank™ accession numbers: DNA: X80075; Protein: 2116232A	Identity: 958/964 (99.4%) a28-g48; c129-a149; c145-t165; c227-t247; t228-c248; t600-c620.	Identity: 312/314 (99.4%) T3-A3; T69-I69.
vs. Brain OGC GenBank™ accession numbers: DNA: NM_022398, U84727 (source); Protein: AAB41797, NP_071793	Identity: 934/943 (99.0%) a28-g7; g160-n139; a182-g161; c189-t168; a433-c412; t600-c579; g698-t677; g785-a764; g958-a937.	Identity: 308/314 (98.1%) T3-A3; K46-N46; T138-P138; S226-I226; G255-E255; G313-S313.
vs. Liver ODC[1] GenBank™ accession numbers: DNA: AJ289714[2] Protein: CAC27716[2]	Identity: No significant homologies.	Identity: 72/266 (27.1%)

[1]ODC, oxodicarboxylate carrier. [2]The carrier cDNA with accession number AJ289714 is listed in GenBank™ as the rat mitochondrial oxodicarboxylate carrier. It is described in the original reference (Fiermonte et al., 2001) as an exchanger that transports 2-OG as well as several other C2-C5 dicarboxylates. mRNA for the carrier was detected by RT-PCR in mitochondria of rat liver, kidney, heart, lung, spleen, testes, skeletal muscle, and brain. The protein was detected by immunodetection in mitochondria of rat heart, kidney, liver, lung, spleen, and brain. The relationship of the ODC with the OGC, however, is unclear.

JPET Fast Forward. Published on November 15, 2005 as DOI: 10.1124/jpet.105.094599
This article has not been copyedited and formatted. The final version may differ from this version.

Table 2. Comparison of kinetic parameters for transport of 2-OG and GSH by bacterial-expressed, purified and reconstituted OGC-WT and OGC-C221,224S.

Uptake rates of 2-OG and GSH for the WT and double-cysteine mutant carriers were derived from Eadie-Hofstee plots of 1-min uptake rates derived from data shown in Figures 2 and 3.

		OGC-WT	**OGC-C221,224S**
2-OG			
	K_m (mM)	0.18 ± 0.03	2.45 ± 0.42
	V_{max} (nmol/min per mg protein)	475 ± 37	143 ± 22
	V_{max}/K_m	2639	58.4
GSH			
	K_m (mM)	1.25 ± 0.15	1.43 ± 0.22
	V_{max} (nmol/min per mg protein)	375 ± 42	70.2 ± 10.5
	V_{max}/K_m	300	49.1

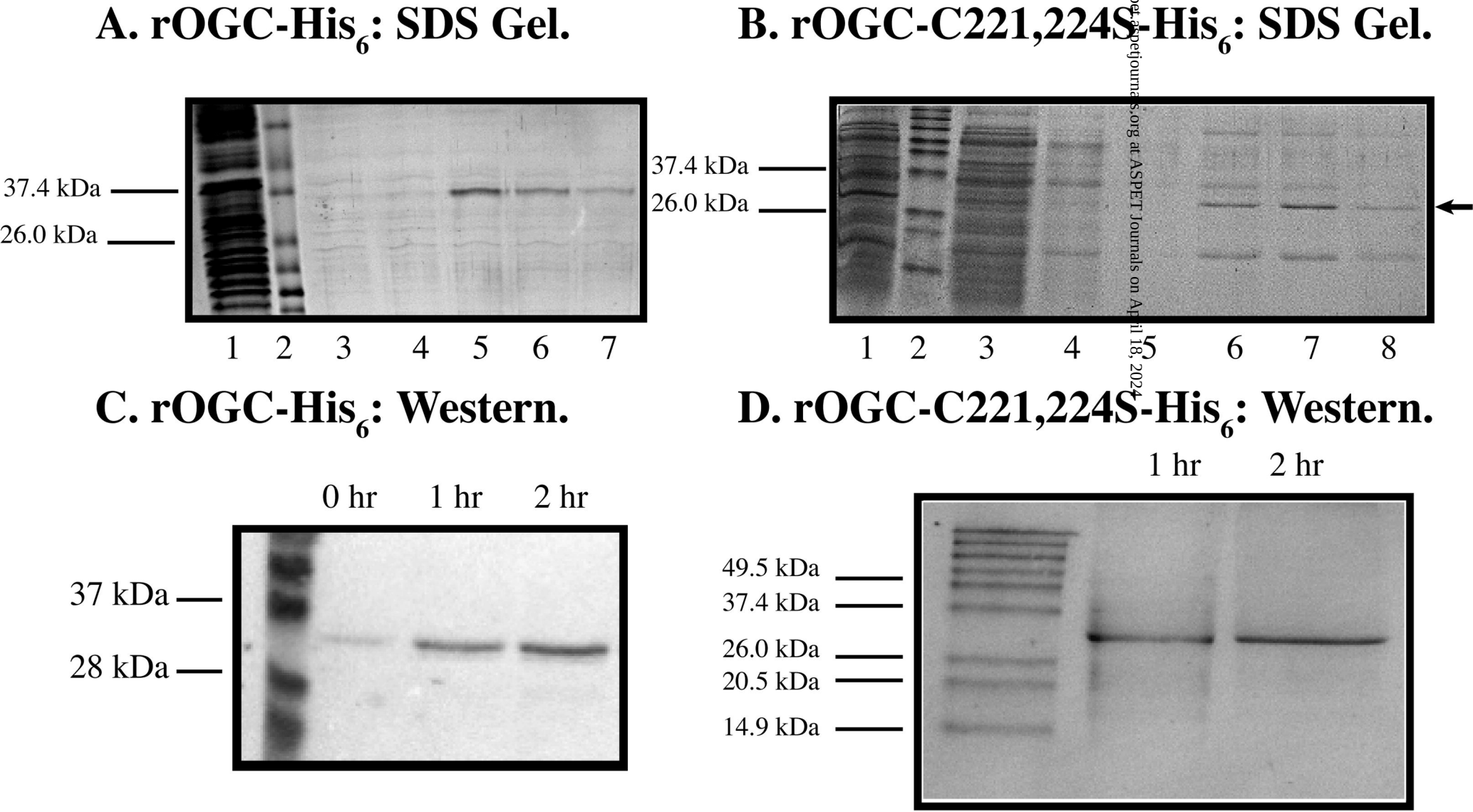

Figure 1. Xu et al.

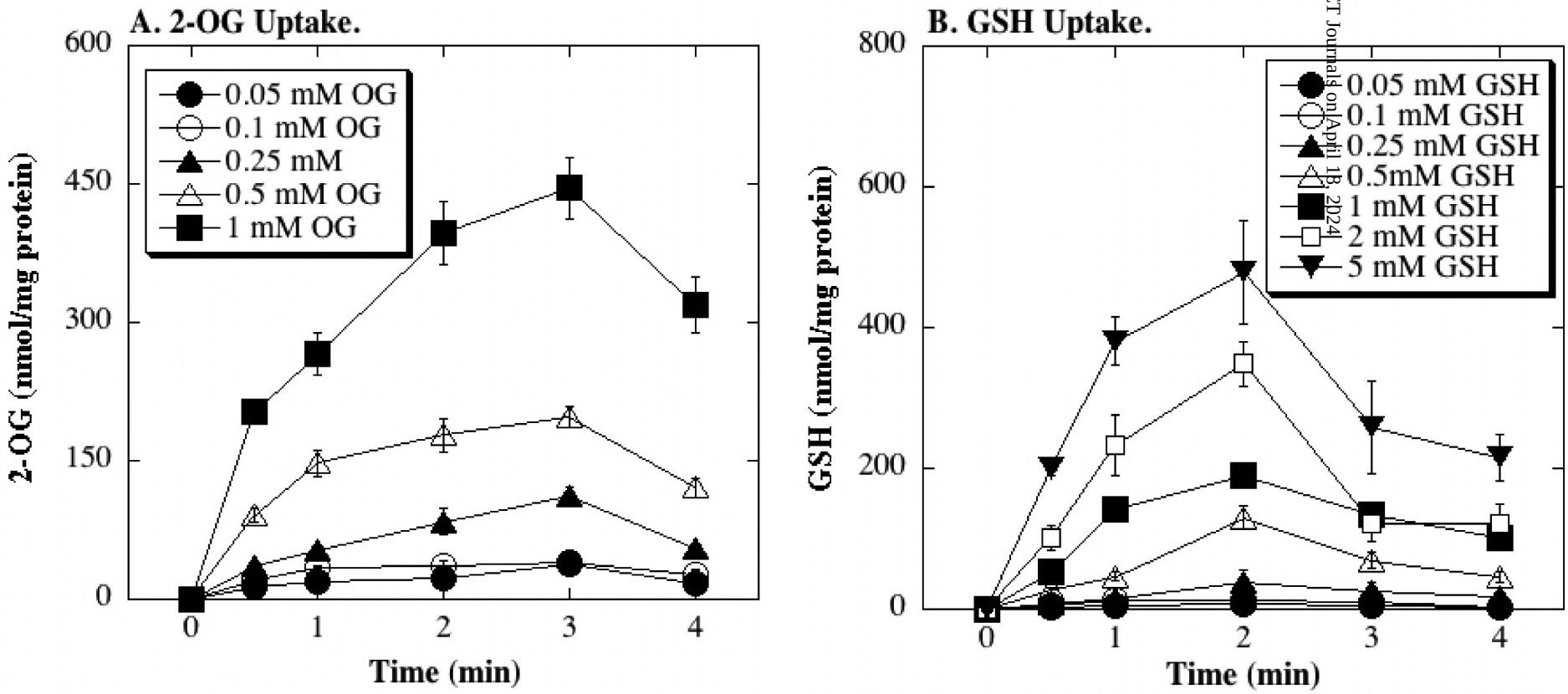

Figure 2. Xu et al.

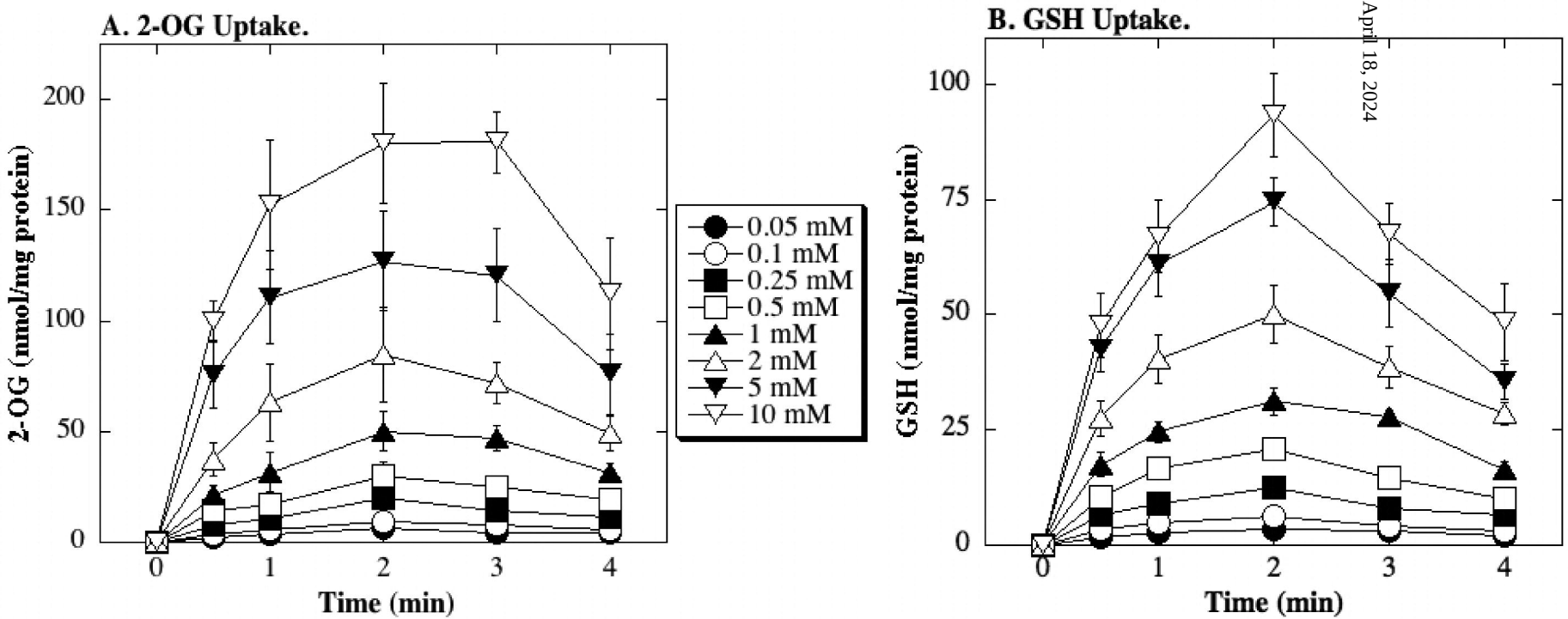

Figure 3. Xu et al.

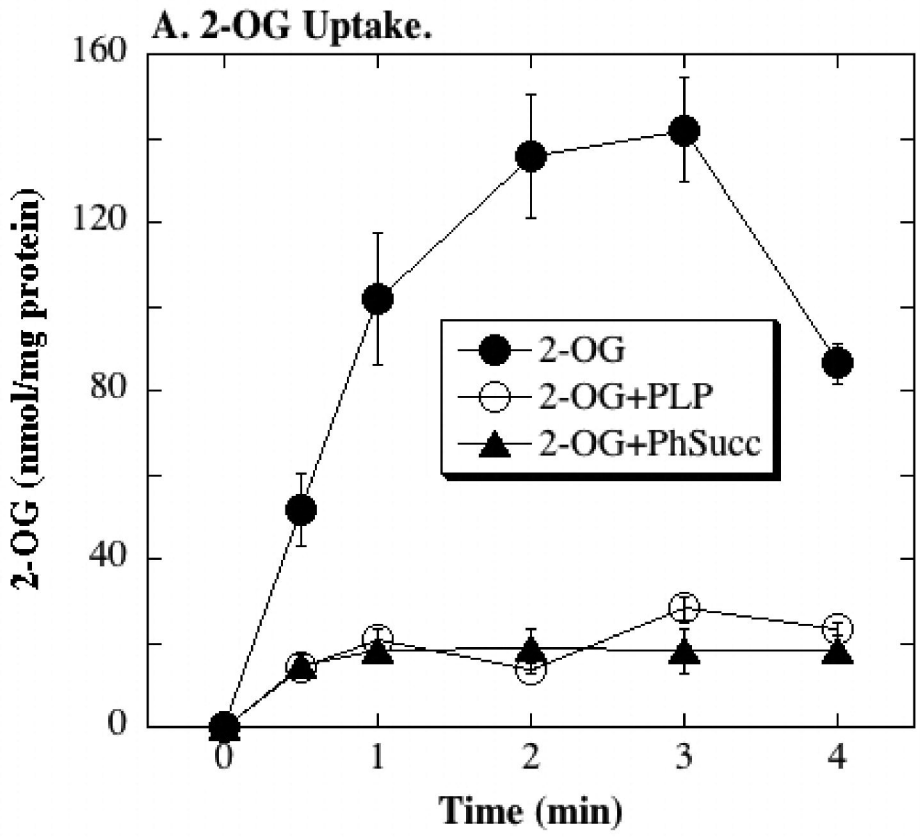

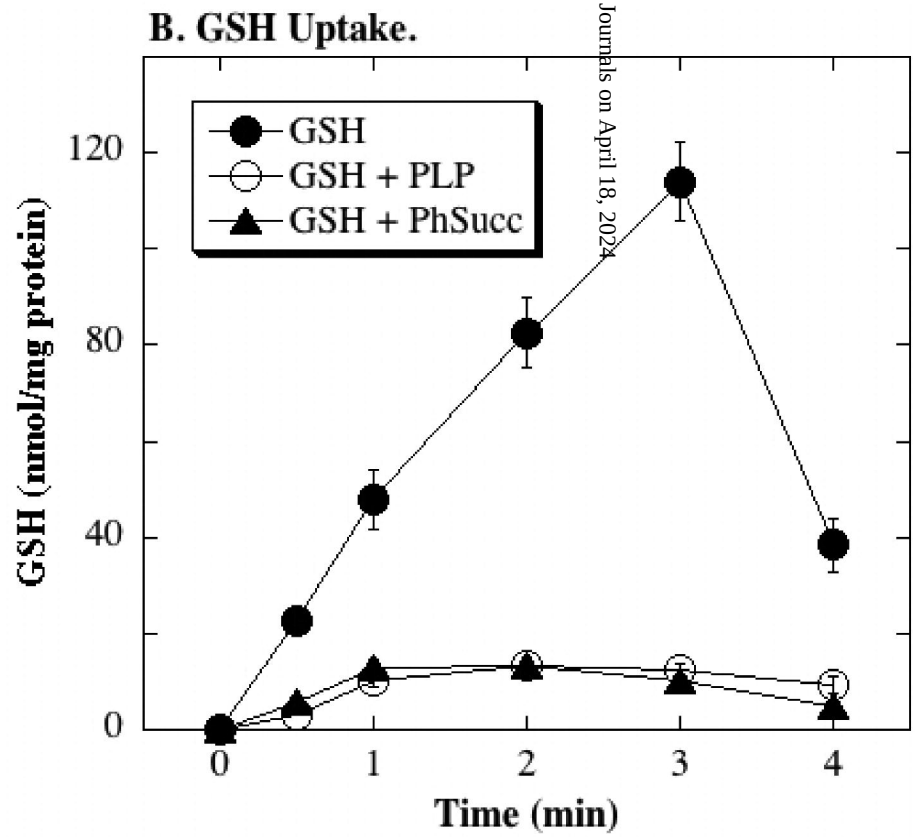

Figure 4. Xu et al.

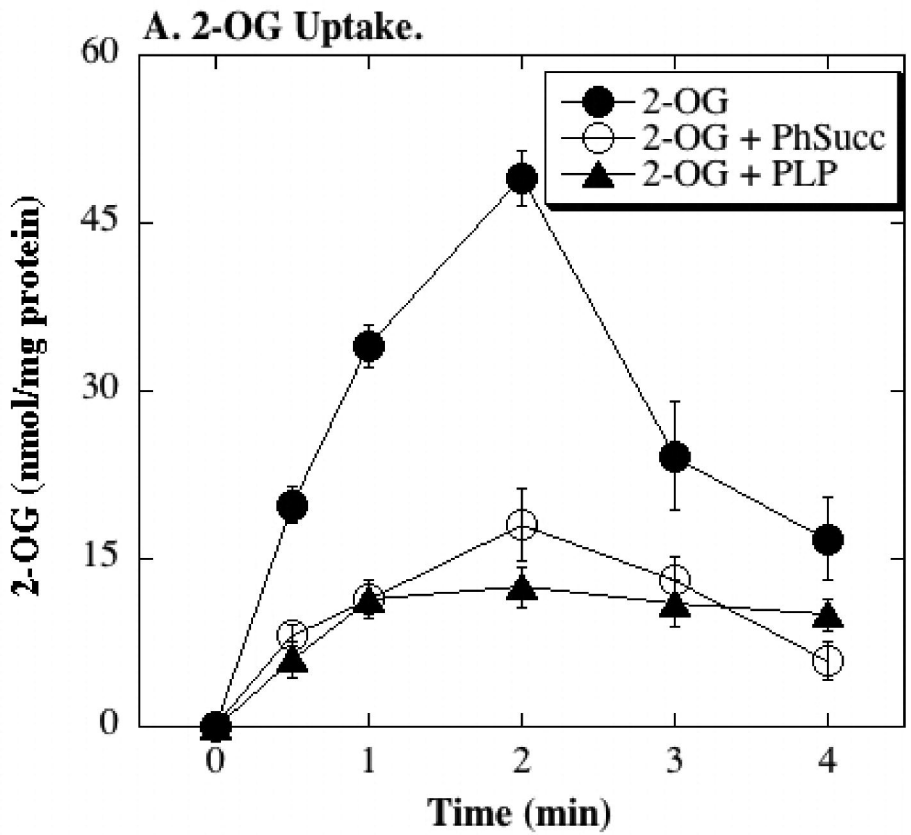

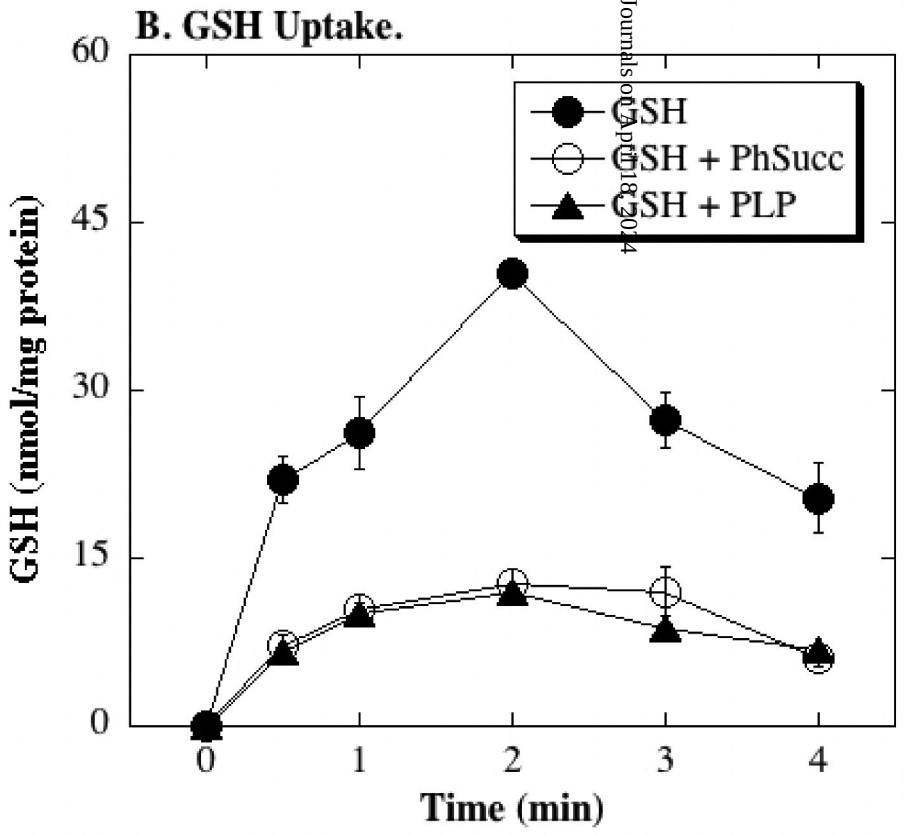

Figure 5. Xu et al.

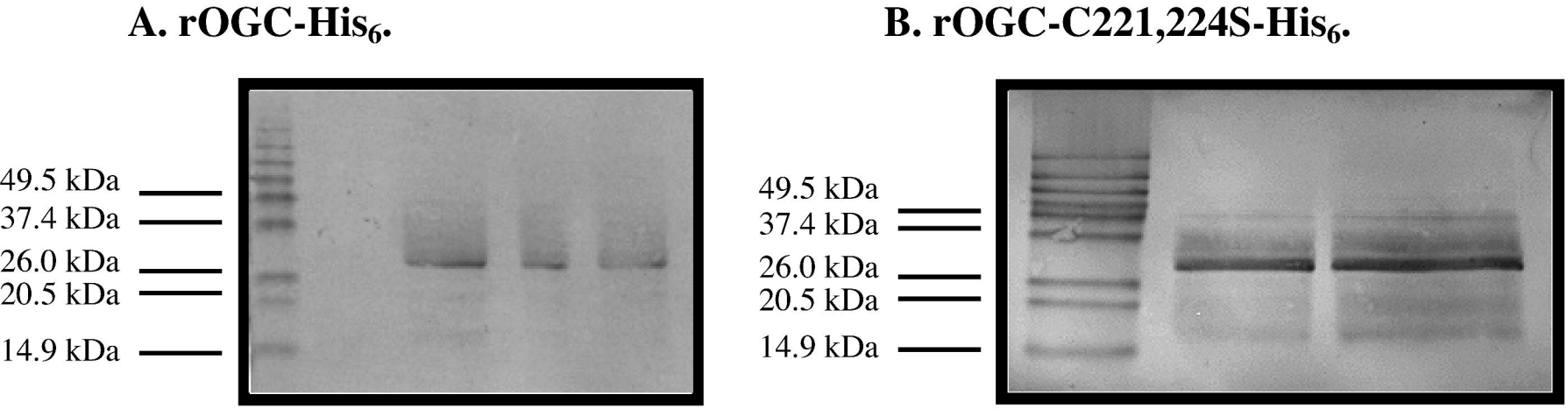

Figure 6. Xu et al.

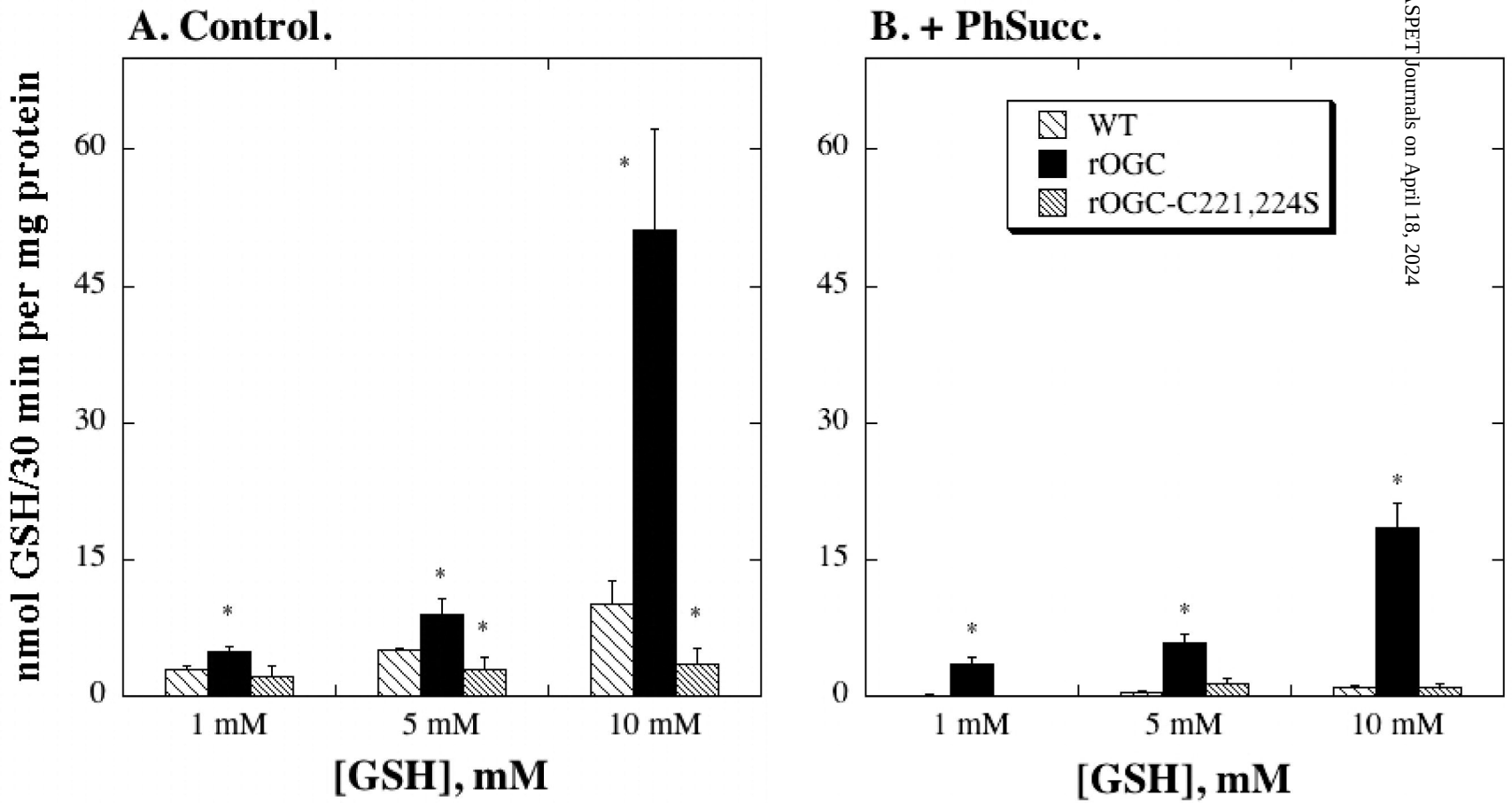

Fig. 7. Xu et al.

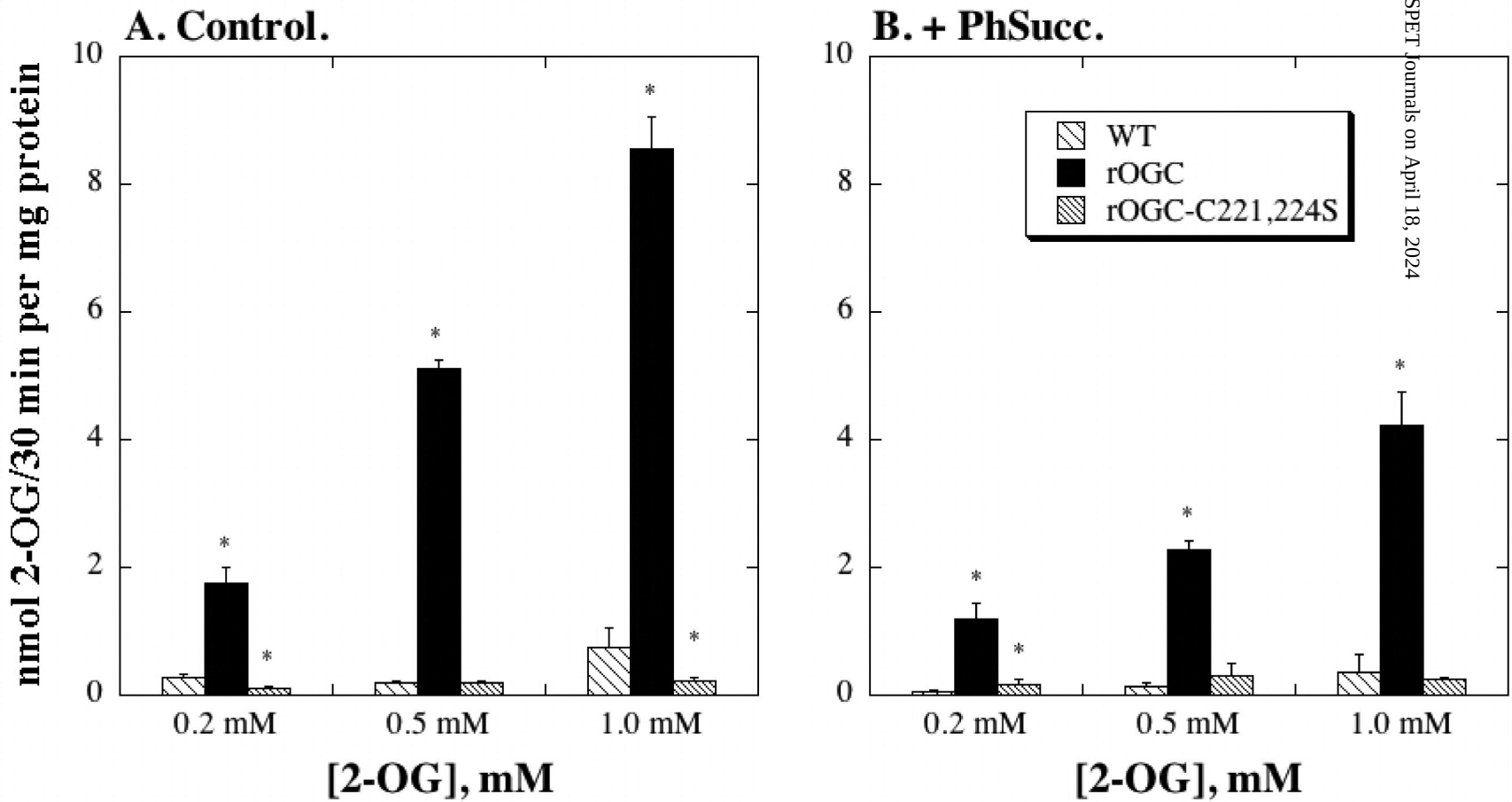

Fig. 8. Xu et al.

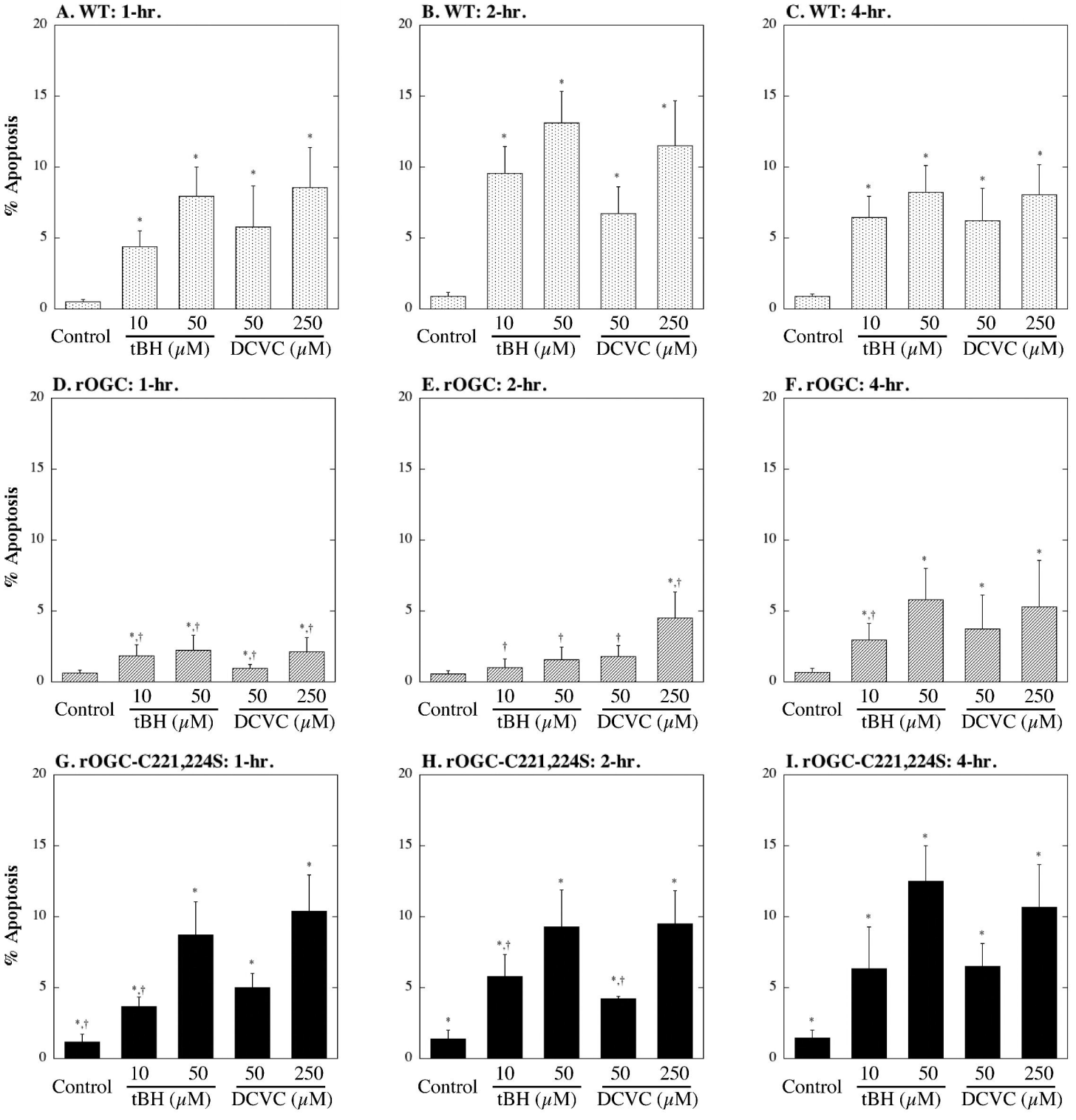

Figure 9. Xu et al.